Research Article

A CANDIDATE GSSP FOR THE BASE OF THE ANISIAN FROM KÇIRA, ALBANIA

Giovanni Muttoni[1]*, Alda Nicora[1], Marco Balini[1], Miriam Katz[2], Morgan Schaller[2], Dennis V. Kent[3], Matteo Maron[1], Selam Meço[4], Roberto Rettori[5], Viktor Doda[6], and Shaquir Nazaj[4]

[1]*Dipartimento di Scienze della Terra 'Ardito Desio', via Mangiagalli 34, 20133 Milan, Italy.*
[2]*Department of Earth and Environmental Sciences, Rensselaer Polytechnic Institute, Troy, New York, 12180, USA.*
[3]*Earth and Planetary Sciences, Rutgers University, Piscataway, New Jersey, USA and Paleomagnetics Lab, Lamont-Doherty Earth Observatory, Palisades New York 10964, USA.*
[4]*Faculty of Geology and Mining, Tiranë, Albania.*
[5]*Dipartimento di Scienze della Terra, Piazza Università, 06100 Perugia, Italy.*
[6]*Albanian Geological Survey, Myslym Keta, Tiranë, Albania.*

*Corresponding author, *Email: giovanni.muttoni1@unimi.it*

Abstract– We present a summary of previously published Olenekian–Anisian boundary magnetostratigraphic and biostratigraphic results from the Kçira area of northern Albania. We focus on the stratigraphically complete Kçira-A section that represents a potential candidate Global Boundary Stratotype Section and Point (GSSP) for the base of the Anisian Stage of the Triassic System. The previously published conodont biostratigraphy from Kçira-A and ancillary sections located nearby has been updated using modern taxonomic criteria and correlated to the available ammonoid and benthic foraminifera biostratigraphy. Previously published magnetobiostratigraphic data reveal the occurrence at Kçira-A, and ancillary sections, of a well-defined magnetic polarity reversal pattern of primary origin that allows global correlations ensuring the exportability of biostratigraphic datums (e.g., the first occurrence of conodont *Chiosella timorensis*) falling close to the Kclr/Kc2n polarity transition. A suite of pilot samples has also been studied for bulk carbon and oxygen isotopes stratigraphy, yielding reasonable values that suggest good preservation of primary material. These data indicate that with additional studies, Kçira-A would represent an ideal base Anisian GSSP.

INTRODUCTION

Arthaber (1911) and Nopcsa (1929) first described an Early Triassic ammonoid fauna within a reddish nodular limestone succession from the Kçira area of northern Albania. In this area, Muttoni et al. (1996) reported a detailed magnetostratigraphic record of an Olenekian/Anisian boundary section termed Kçira-A that was correlated to the vertical distribution of key conodonts (figured by Meço, 2010 and reported also below), ammonoids, and benthic foraminifera species. Ancillary sections from the same nodular limestone unit were also studied for magneto-biostratigraphy (Kçira-B) and magnetostratigraphy (Kçira-C), and were correlated to the reference Kçira-A section. Ammonoids from Kçira-A and a further ancillary section (Kçira-G) were appraised by Germani (1997). A geologic map of the Kçira area (Muttoni et al., 1996) was recently augmented by additional biostratigraphic and tectonic observations and data (Gawlick et al., 2008, 2014, 2016), which complements geologic studies of Albania (Meço, 2000 and references therein). These studies reveal that the thicker and stratigraphically more complete Kçira-A section has excellent potential as a candidate Global Boundary Stratotype Section and Point (GSSP) for the base of the Anisian Stage of the Triassic System. In this paper, we summarize key magneto-biostratigraphy aspects of Kçira-A and ancillary sections,

Published online: August 2, 2019

Muttoni, G., Nicora, A., Balini, M., Katz, M., Schaller, M., Kent, D., Maron, M., Meço, S., Rettori, R., Doda, V., & Nazaj, S.. 2019. A candidate GSSP for the base of the Anisian from Kçira, Albania. *Albertiana*, vol. 45, 39–49.

describe new carbon and oxygen isotope results, and discuss future developments aimed at formally proposing Kçira-A as candidate Anisian GSSP.

GEOLOGY AND LITHOSTRATIGRAPHY

Kçira is located in northern Albania about 130 km (2.5 hours by car) north of Tirana. This area is characterized by a complex mélange of blocks, ranging in size from a few meters to some kilometers, comprised of Early to Late Triassic limestones, Triassic volcanics, and Triassic radiolarites, embedded in a thick Bathonian–Callovian (Jurassic) radiolaritic-ophiolitic unit (Fig. 1A) (Gawlick et al., 2008, 2014, 2016; Gaetani et al., 2015). The Kçira-A section crops out to the northwest of the new Kçira village (Fig. 1A, B, C), together with additional ancillary sections described in this study, that have been correlated by means of lithostratigraphy, magnetostratigraphy, and biostratigraphy (Fig. 2) as discussed below. These sections are part of an Olenekian–Anisian nodular limestone belt that probably formed as a single slab prior to being embedded into the Jurassic radiolaritic-ophiolitic unit. This tectonic mélange is part of the Kçira-Dushi-Komani radiolaritic flysch (ophiolitic Mélange) at the sole of the Mirdita Zone ophiolites (Gaetani et al., 2015; Gawlick et al., 2016 and references therein).

The Kçira-A (main) section is about 42 m thick, whereas the ancillary Kçira-B section, located a few meters away within the same outcrop, is about 4.5 m thick. On the basis of magnetostratigraphic correlation, projected layers of Kçira-B partially overlap with the basal portion of Kçira-A (Fig. 2). As reported in Muttoni et al. (1996), both sections are comprised of reddish to pale pink wackestones and mudstones arranged in cm thick nodular beds that are strongly amalgamated to form meter-scale composite layers. These limestones were termed the Han-Bulog Limestone by Muttoni et al. (1996), but red nodular limestones of the Bulog Formation in southwest Serbia are Anisian in age and developed on top of a drowned Middle Anisian (Pelsonian) shallow-water carbonate ramp (Sudar et al., 2013). Therefore, as proposed by Gawlick et al. (2014), the Olenekian–Anisian red nodular limestones of Kçira (rosenrot Knollenkalk of Nopcsa, 1929 equivalent to the Han-Bulog Limestone of Muttoni et al., 1996) should not be termed Bulog (or Hallstatt, or Han-Bulog) Limestone, at least in the Olenekian section. We

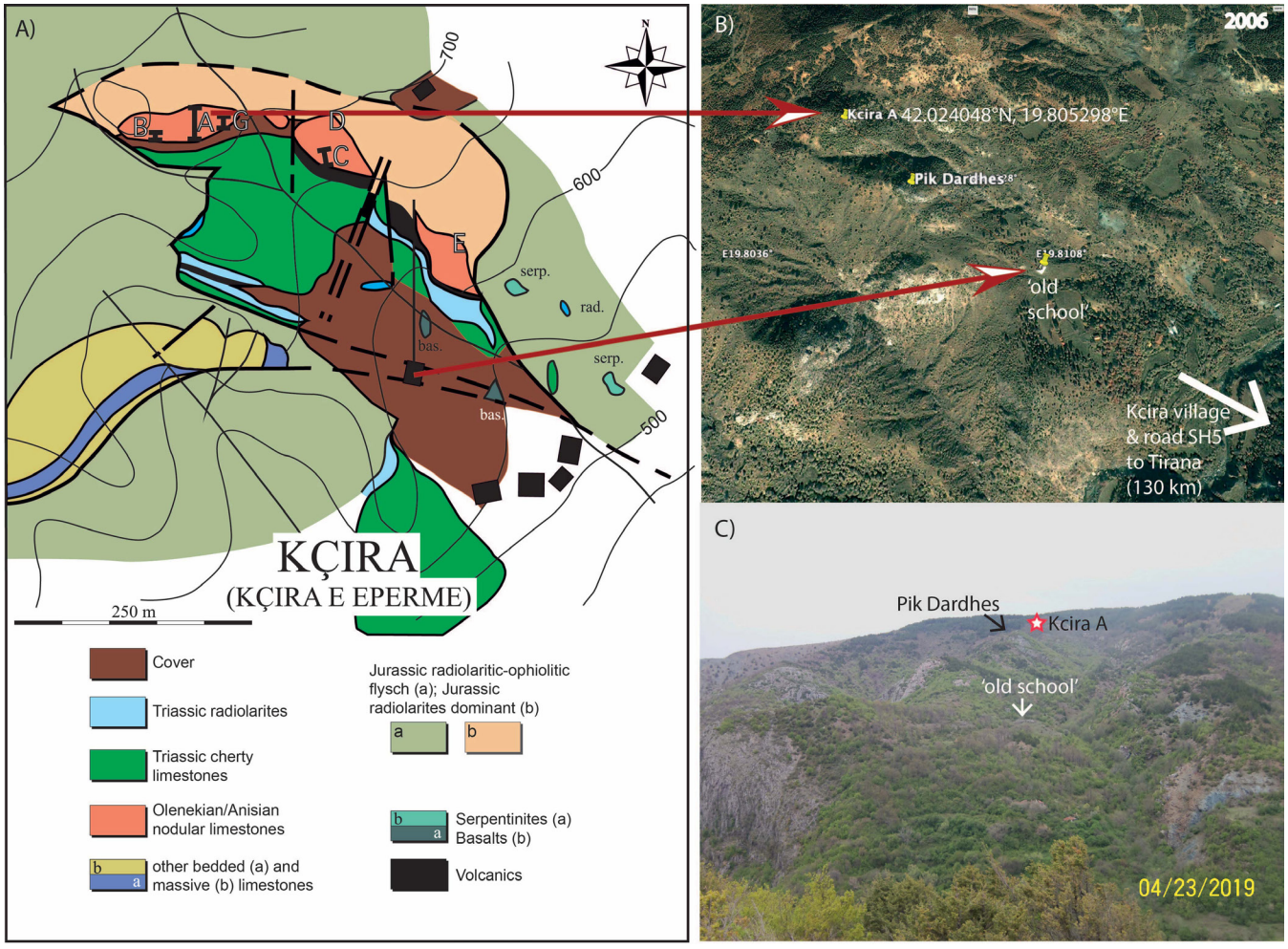

Figure 1 – *A*, Geological map of the Kçira area (modified after Muttoni et al., 1996 using data from Gawlick et al., 2014). 'A', 'B', 'C', 'G' are sections Kçira-A, Kçira-B, Kçira-C, and Kçira-G; 'D' and 'E' are additional sites of paleontological or lithological interest described in Muttoni et al. (1996). *B*, Aerial view and *C*, picture of the Kçira area with location of conspicuous points and the Kçira-A GSSP candidate.

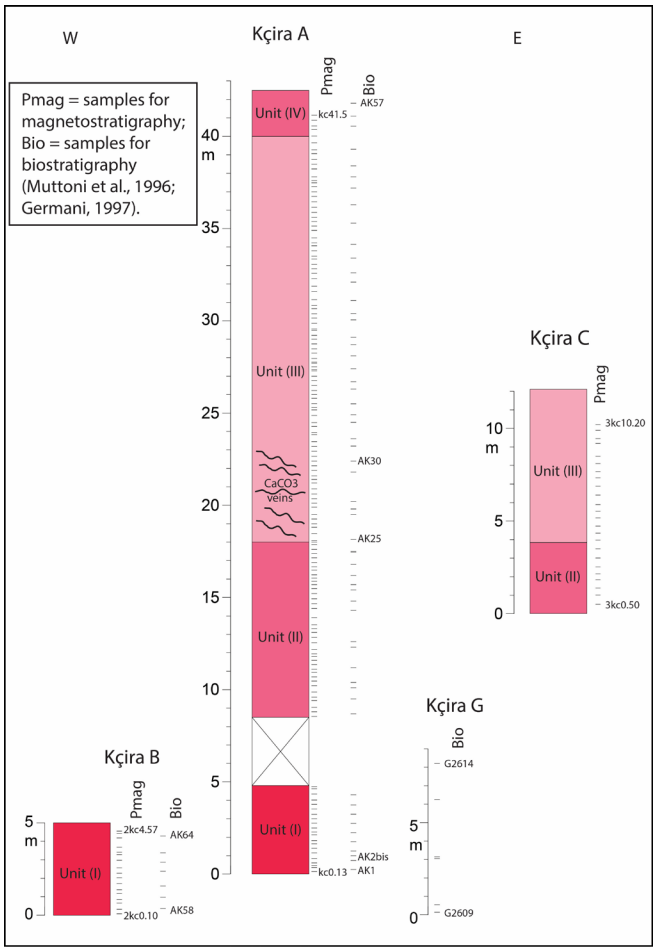

Figure 2 – Main lithological units of the correlated Kçira sections discussed in the text with position of paleomagnetic (Pmag) and biostratigraphic (Bio) samples after Muttoni et al. (1996) and Germani (1997).

provisionally and informally refer to these Olenekian–Anisian limestones as nodular limestones of Kçira.

The basal 4.8 m of nodular limestones at Kçira-A (as well as the entire Kçira-B) are reddish and clay-rich, with pervasive bedding-parallel stylolites (lithologic Unit I, Fig. 2). Above a cover extending up to meter level 8.5, amalgamated nodular limestones become pink (Unit II) and then pale pink (Unit III) (Fig. 2). A set of cm thick calcite veins cut the bedding between meter 18 and 23 at Kçira-A. The uppermost few meters of Kçira-A contain packstones, which are more pink, richer in bioclasts, and are more distinctly bedded (Unit IV, Fig. 2). The top of the Kçira nodular limestone is marked by small neptunian dikes sealed by a cm thick silicified crust of uncertain age, as observed at site D (Fig. 1A).

The Kçira-C section is 10.2 m thick and located about 100 m east of Kçira-A and Kçira-B (Fig. 1A). Although a detailed lithological description was not made for Kçira-C, an upsection decrease in red pigmentation to pink closely resembles that observed at Kçira-A (Fig. 2), which provides a first order means of lithological correlation (Muttoni et al., 1996). Kçira-G is located in between Kçira-A and Kçira-C (Fig. 1A), but no lithological description is provided (Germani, 1997). Based on projected layers, Kçira-G should correspond to the basal Kçira-A as well as the entire Kçira-B sections (Fig. 2).

Two sections were previously studied for magnetostratigraphy and biostratigraphy (Kçira-A and Kçira-B; Muttoni et al., 1996), Kçira-C only for magnetostratigraphy (Muttoni et al., 1996), and Kçira-G only for biostratigraphy (Germani, 1997). The Kçira-A and Kçira sections are most likely the localities described by Nopcsa (1929). Bedding attitude (azimuth of dip/dip) varies from 347°E/34° at Kçira-A to 12°E/45°E at Kçira-B and Kçira-C.

BIOSTRATIGRAPHY

Conodonts

Conodonts from Kçira-A and Kçira-B sections originally reported by Muttoni et al. (1996) have been revised in this study according to recent advances in conodont taxonomy. Some conodont species of Muttoni et al. (1996) were later illustrated by Meço (2010) and are reported in Figure 3. The conodont fauna from these sections is abundant and well preserved. The CAI (Color Alteration Index, Epstein et al., 1977) is 3, indicating that the host rock reached burial temperatures of 110°–200°C. The conodont main events are grouped as follows from the base to the top (Fig. 4; see also key species in Fig. 3):

1. The conodont association from lithologic Units I and II is represented by *Triassospathodus abruptus* Orchard, 1995, *T. triangularis* (Bender, 1970), *Spathicuspus spathi* (Sweet, 1970), *T. homeri* (Bender, 1970), *Gladigondolella carinata* Bender, 1970, *T. symmetricus* (Orchard, 1995), *T. brochus* (Orchard, 1995), *Neogondolella* sp., *N.* sp. A, *Triassospathodus* sp., and *Gladigondolella tethydis* (Huckreide, 1958). This fauna is mostly consistent with fauna 3 of Orchard (1995) and with the fauna described in the lower part of the Deşli Caira section (North Dobrugea, Romania) by Gradinaru et al. (2007) and Orchard et al. (2007a), as well as in the Lower Guandao section (Guizhou Province, China) by Orchard et al. (2007b). These faunas are altogether attributed to the late mid Spathian.

2. The appearance of *Chiosella gondolelloides* (Bender, 1970) (sample AK28, 20.2 m) is an easily recognized datum that predates the occurrence of *C. timorensis* (Nogami,1968; AK30, 22.4 m). This is in broad agreement with data from Chios (Gaetani et al., 1992; Muttoni et al., 1995), Deşli Caira (Gradinaru et al., 2007; Orchard et al., 2007a) and Lower and Upper Guandao (Orchard et al., 2007b). The appearance of *Chiosella timorensis* (=*Gondolella timorensis* in Gaetani et al., 1992; Muttoni et al., 1995) may be used to approximate the base of the Anisian (Gradinaru et al., 2006, 2007; Orchard et al., 2007a, 2007b) especially when ammonoids are absent. Orchard (1995), Gradinaru et al. (2007), Orchard et al. (2007a, 2007b) have well summarized and described the taxonomy of these species.

3. *Neogondolella regalis* Mosher, 1970 appears at 26.7 m (AK37) and is interpreted to span the late Aegean and mid Bithynian (Mosher, 1970; Gedik, 1975; Nicora, 1977; Kovacs & Kozur, 1980).

4. *Paragondolella bulgarica* Budurov and Stefanov (1975) appears at 28.7 m (AK40) and is a proxy for the base of the Bithynian substage. It ranges up to the boundary interval of the *Binodosus* and *Trinodosus* ammonoid Zones (Budurov & Stefanov,

1972, 1975; Gedik, 1975; Nicora, 1977; Kovacs & Kozur, 1980; Balini & Nicora, 1998; Farabegoli & Perri, 1998; Kovacs & Ralisch-Felgenhauer, 2005; Balini et al., 2019).

5. Nicoraella kokaeli (Tatge, 1956) appears at 35.3m (AK49) and approximates the base of the Pelsonian substage (Nicora, 1977; Kovacs & Kozur, 1980; Balini & Nicora, 1998; Farabegoli & Perri, 1998).

6. Paragondolella bifurcata bifurcata (Budurov and Stefanov, 1972) appears at 33.4 m (AK47) while *P. bifurcata hunbuloghi* Sudar and Budurov, 1979 appears at 35.3 m (AK49). These species are attributed to the Pelsonian substage (Budurov & Stefanov, 1972, 1975; Sudar & Budurov, 1979; Kovacs & Kozur, 1980; Balini & Nicora, 1998; Kovacs & Ralisch-Felgenhauer, 2005).

Based on the conodont fauna, the Kçira-A section covers the late mid Spathian to Pelsonian while Kçira-B section is restricted to the late mid Spathian.

Ammonoids

The lower part of the Kçira-A section (Unit I of Figs. 2–4) is rich in ammonoids. From this part of the section, Germani (1997) described a small fauna with high diversity that is middle Spathian (*Subcolumbites* Zone sensu Guex et al., 2010

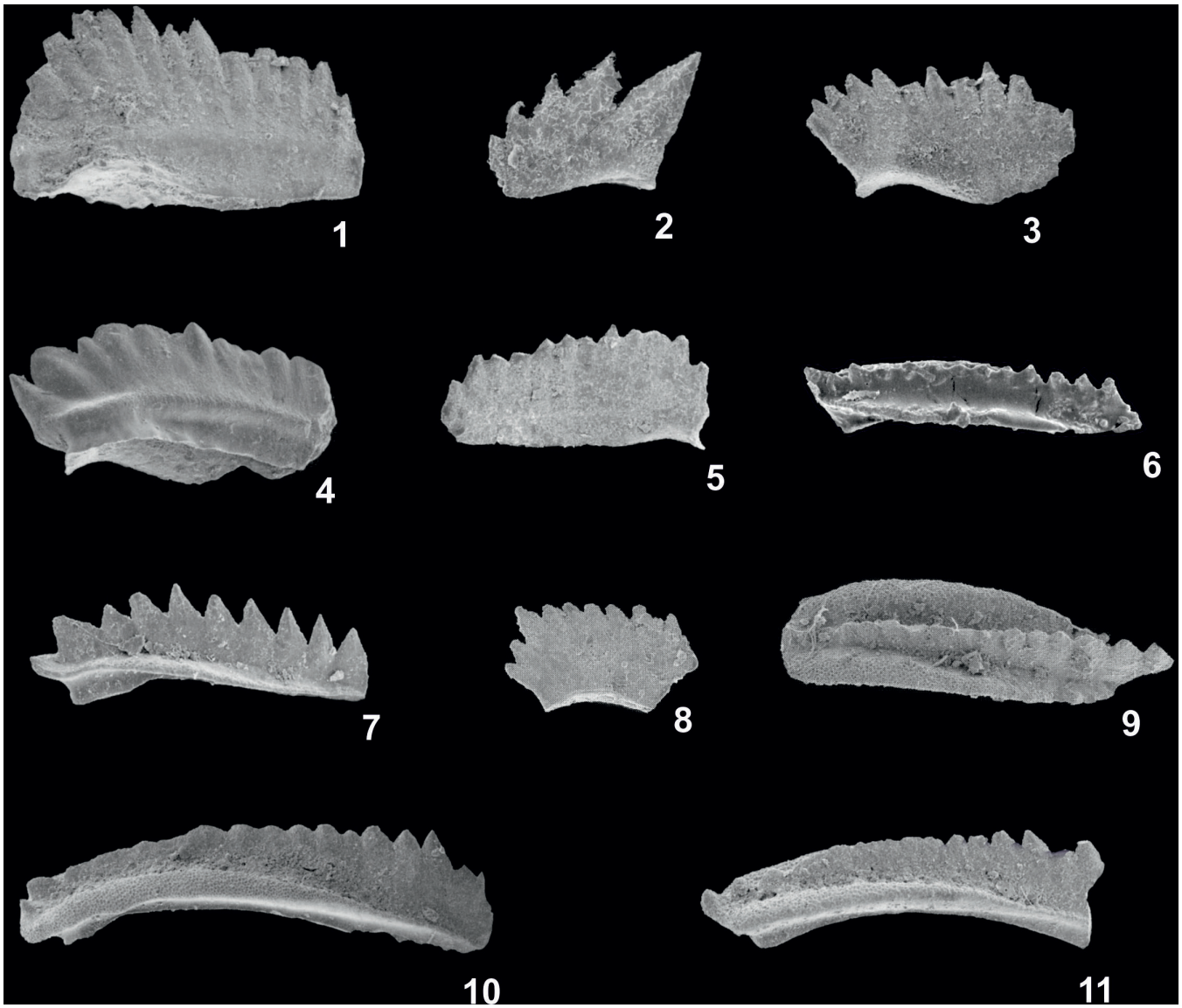

Figure 3 – Conodonts from Kçira-A and Kçira-B of Muttoni et al. (1996), figured in Meço (2010), and taxonomically updated in this study. (1) *Triassospathodus abruptus* Orchard, 1995, lateral view, Kçira-B, sample AK62, x 70. (2) *Spathicuspus spathi* (Sweet, 1970), lateral view, Kçira-A, sample AK13, x 120. (3) *Triassospathodus homeri* (Bender, 1970), lateral view, Kçira-A, sample AK8, x 80. (4) *Chiosella timorensis* (Bender, 1970), lateral view, Kçira-A, sample AK31, x 82. (5) *Chiosella gondolelloides* (Bender, 1970), lateral view, Kçira-A, sample AK35, x 90. (6) *Neogondolella regalis* Mosher, 1970, oblique-upper view, Kçira-A, sample AK37, x 100. (7) *Paragondolella bulgarica* (Budurov & Stefanov, 1972), juvenile stage, lateral view, Kçira-A, sample AK42, x 110. (8) *Nicoraella kokaeli* (Tatge, 1956), lateral view, Kçira-A, sample AK55, x 105. (9) *Paragondolella bifurcata hunbuloghi* (Sudar and Budurov,1979), oblique-upper view, Kçira-A, sample AK52, x 80. (10) *Paragondolella bifurcata bifurcata* (Budurov and Stefanov, 1972), lateral view, Kçira-A, sample AK48, x 80. (11) *Paragondolella bifurcata bifurcata* Budurov & Stefanov, 1972, lateral view, Kçira-A, sample AK48, x 80.

and Jenks et al., 2013). This fauna (Fig. 5) is dominated by *Subcolumbites* and *Albanites*, in addition to leiostraceans, and is almost equivalent to the fauna described from Kçira by Arthaber (1911). Ammonoid assemblages also indicate middle Spathian at Kçira-B and Kçira-G (Germani, 1997). Ammonoids also are reported from the middle and upper part of the Kçira-A section (Germani, 1997) in Units III and IV (Fig. 5), but they are long-ranging leiostracean that verify the presence of Anisian strata, but thus far a more refined age assignment is not possible.

Benthic Foraminifera

As outlined in Muttoni et al. (1996), benthic foraminifera are very scarce in the lower part of Kçira-A (Fig. 5). *Gaudryina*? n. sp. is discontinuously present from meter 14.3 (AK17) to 22.4 (AK30), where *Meandrospira dieneri*? appears. A more diversified and abundant fauna was recovered from meter 28.1 to 34.2 at Kçira-A (samples AK39 to AK48). This assemblage is characterized by *Ophtalmidium* aff. *O. abriolense*, *Arenovidalina chialingchiangensis, Pilammina densa*, *Meandrospira dinarica*, *Earlandia amplimuralis* and *E. gracilis*. An Anisian age not younger than Pelsonian is attributed to this assemblage. It is noteworthy that *P. densa* occurs in association with conodonts of Bithynian age.

PALEOMAGNETISM

Paleomagnetic properties

Samples for paleomagnetic analyses were collected with a portable water-cooled rock drill and oriented with a magnetic compass. Sections Kçira-A and Kçira-B were sampled at an average interval of 20–25 cm, while sampling at 40–50 cm was applied at Kçira-C (Fig. 6; Muttoni et al., 1996). Based on standard rock-magnetic experiments, Muttoni et al. (1996) concluded that nodular layers of the lower half of Kçira-A (Units I–II), as well as of Unit I of Kçira-B, were characterized by abundant hematite, contributing to the relatively high natural remanent magnetization (NRM) (Fig. 6A) and magnetic susceptibility, as well as the pervasive reddish-pink hues typical of this part of the succession. In contrast, pale-pink nodular layers above (Unit III) preserve a mineralogical association of less abundant magnetite coexisting with hematite, giving lower NRM and magnetic susceptibility, although the lowest values between meter 18 and 23 at Kçira-A are also associated with a dense network of calcite veins (Fig. 6A). The top of Unit III has a few samples with very high NRM intesities and univectorial component trajectories during thermal demagnetization that are interpreted as due to lightning-induced IRM (Isothermal remanent magnetization), whereas the uppermost few meters of the Kçira succession (Unit IV) are richer in resedimented carbonate layers that might have enhanced the concentration of detrital magnetite (see Muttoni et al., 1996 for details).

Upon application of thermal demagnetization, a characteristic (Ch) component with either northeast-and-down or southwest-and-up directions was resolved in 88% of the samples in the temperature range between about 400°C and either 520–575°C or 650–680°C (Fig. 7A). These Ch component directions display variable mean angular deviation (MAD; Fig. 6B) values depending on NRM intensities (Fig. 6A). They show dual polarity at all investigated sections (Fig. 7B), albeit the normal and reverse mean polarity directions depart from antipodality by up to 27°, perhaps due to contamination of the Ch magnetizations by an initial viscous component broadly aligned along the present-day field direction (Fig. 7A). The three mean directions from Kçira-A, Kçira-B, and Kçira-C (Fig. 7B) show some degree of convergence after correction for bedding tilt, the Fisher precision parameter k increasing by a factor of 3 with a full (100%) tilt correction, suggesting that the Ch magnetizations were acquired before deformation. However, the limited difference in bedding attitudes makes the fold test statistically inconclusive (see Muttoni et al., 1996 for details).

Magnetostratigraphy and correlations with sections from the literature

A virtual geomagnetic pole (VGP) was calculated for each sample Ch component direction after correction for bedding tilt. The latitude of the sample VGP with respect to the overall mean (north) paleomagnetic pole (i.e. VGP latitude) was used to delineate the magnetic polarity stratigraphy (Fig. 6C, D). At Kçira-A, the VGP latitudes define a sequence of polarity intervals extending from Kc1n.1n at the base to Kc3r at the top. Submagnetozone Kc1n.1r near the base of Kçira-A nicely correlates to the short reverse polarity interval at Kçira-B, lending credibility to this single sample-based reversal. Finally, the magnetic polarity stratigraphy at Kçira-C shows an excellent match with Kçira-A across multiple polarity reversals in the Kc1r interval (Fig. 6), which also contain several biostratigraphic events potentially useful to define the base of the Anisian.

According to the recent Triassic geomagnetic polarity scale of Maron et al. (2019), the magnetostratigraphic sequence of Kçira-A correlates reasonably well with the Lower and Upper Guandao (Lehrmann et al., 2015), Chios (Muttoni et al., 1995), and Desli Caira (Gradinaru et al., 2007) sections (see Figures 11 and 12 in Maron et al., 2019). According to this correlation scheme that incorporates U-Pb age data from Guandao (Lehrmann et al., 2015), Kçira-A should extend from approximately 248 to 244 Ma, and the level containing the appearance of *Chiosella timorensis* should have an interpolated age of ~247.3 Ma (Lehrmann et al., 2015; see also Maron et al., 2019).

CHEMOSTRATIGRAPHY

Carbon isotope stratigraphy provides additional means to correlate among marine sections, and under the right circumstances (and with the independent magnetostratigraphic constraints above) can allow correlation between terrestrial and marine sections (see review by Salzman & Thomas, 2012). The $\delta^{13}C_{carb}$ of bulk sedimentary carbonate can be an important tool to use in sections that lack sufficient biomagnetostratigraphy, especially in older time periods (e.g., Paleozoic, Cramer and

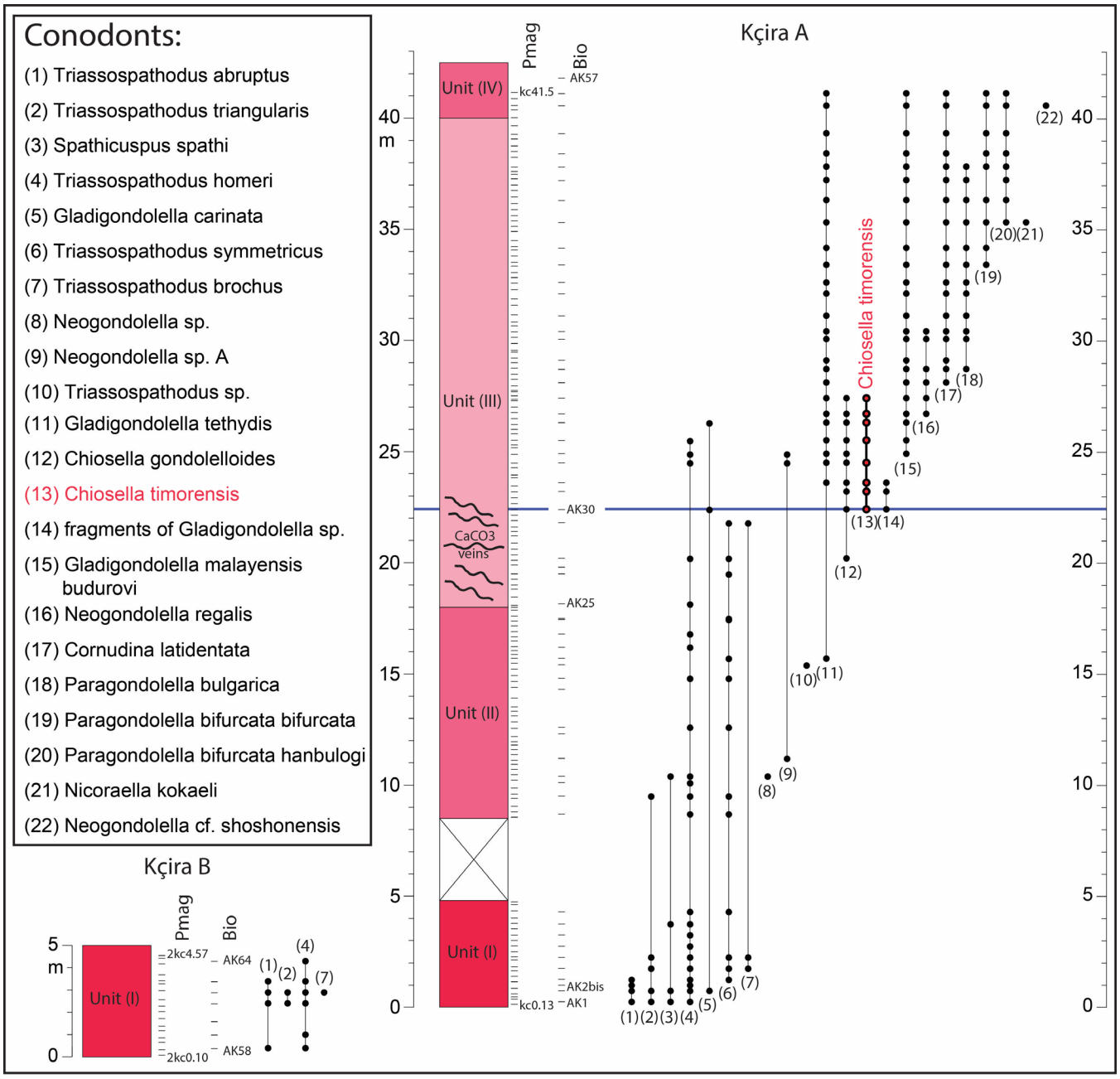

Figure 4 – Vertical distribution of conodonts from Kçira-A and Kçira-B after Muttoni et al. (1996) with taxonomic revision from this study (see also Fig. 3 for pictures of key conodonts).

Saltzmann, 2005; Middle–Late Triassic, Muttoni et al., 2014). The detailed biomagnetostratigraphic framework at Kçira will provide the necessary context to identify and constrain useful carbon isotopic events and trends associated with the base of the Anisian, which then can be used as a template for carbon isotope stratigraphy elsewhere. The Olenekian–Anisian boundary interval is known to contain carbon isotope excursions (e.g., Richoz et al., 2007) that, by virtue of their large amplitudes and global nature, represent useful markers for the base of the Anisian. Therefore, we will analyze carbon stable isotopes on bulk $CaCO_3$ from the Kçira section, and the attendant oxygen isotopes will be used as a metric of the degree of diagenetic alteration (in general, carbon isotopes of calcite are more resistant to diagenetic alteration than oxygen isotopes [Marshall, 1992]).

We conducted a pilot study of bulk carbonate stable isotopes ($\delta^{18}O$, $\delta^{13}C$) using rock samples that were prepared with a Buehler Isomet low speed saw to avoid veins. These selected samples were broken into millimeter fragments using a rock hammer, and then crushed for 15 to 20 minutes, or until completely powdered, at low speed in a Fritsch Ball Mill or an Across International HQ-NO4 Vertical Planetary Ball Mill. Between each crushing, the agate bowl (lid, rubber washer, and cup) was cleaned and rinsed thoroughly to remove any remaining powdered sample. Stable isotopes were measured on bulk sediment samples in the Stable

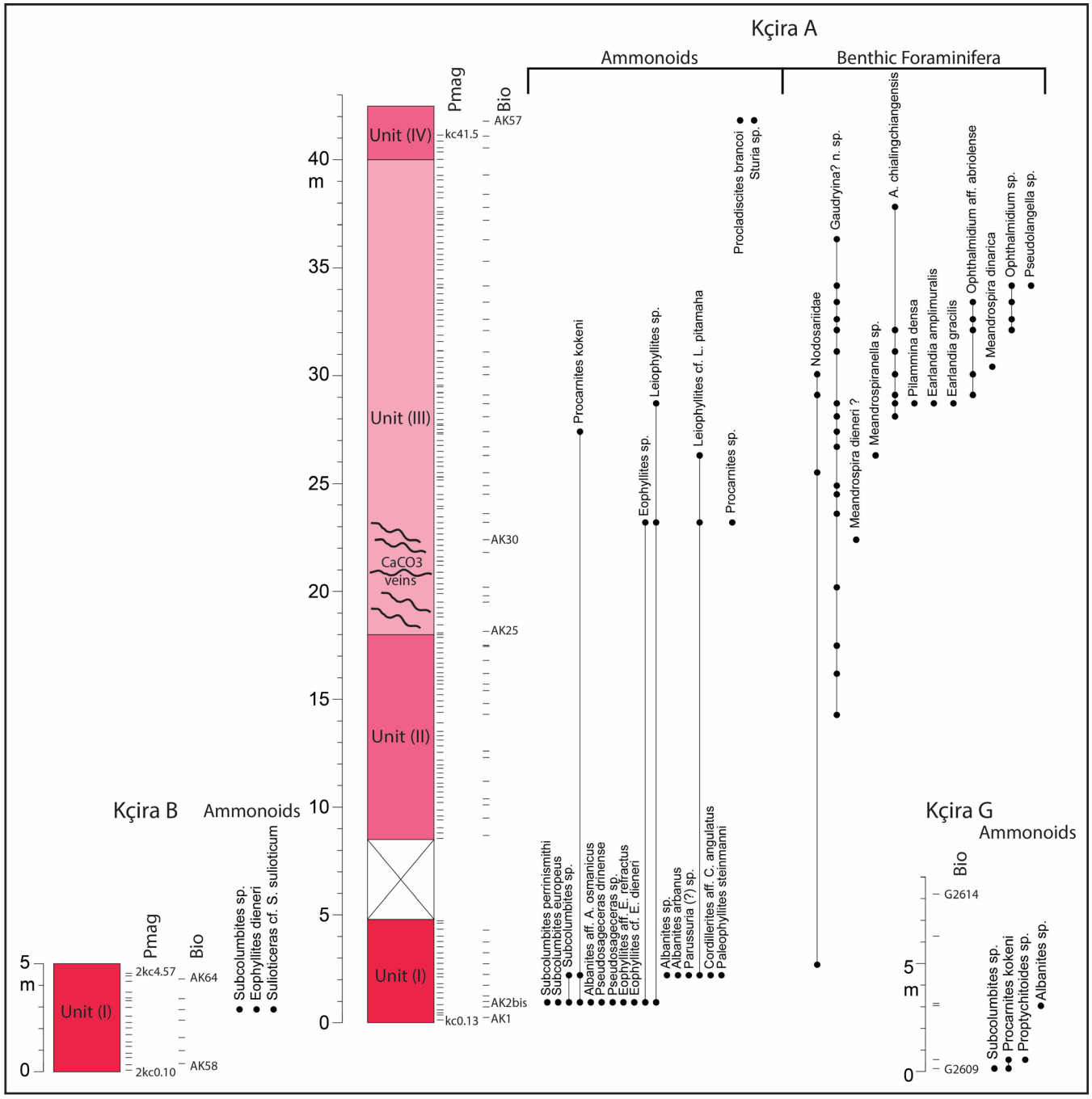

Figure 5 – Vertical distribution of ammonoids from Kçira-A, Kçira-B, and Kçira-G after Germani (1997), and of benthic foraminifera from Kçira-A after Muttoni et al. (1996).

Isotope Lab at Rutgers University using a multiprep peripheral device and analyzed on an Micromass Optima mass spectrometer. Samples were reacted in 100% phosphoric acid at 90°C for 13 min. Values are reported relative to V-PDB through the analysis of an internal standard calibrated with NBS-19 (1.95‰ for $\delta^{13}C$), as reported by Coplen (1995).

Our pilot study of bulk sedimentary $CaCO_3$ shows that Kçira-A samples yield reasonable values, and the $\delta^{18}O$ is consistent with an expected marine range (e.g., see Veizer and Prokoph, 2015), indicating good preservation of primary material (Fig. 8). In particular, the pilot bulk $\delta^{18}O$ is comparable to that of conodont bioapatite (Trotter et al. 2015) that show correlative temperature changes with pCO_2 in the Late Triassic (Knobbe and Schaller 2018). Because of the broadly similar diagenetic and tectonic histories of these sections, we can expect similar results for the Anisian. Relatively little sedimentary carbonate is produced in deep waters, and therefore bulk sediment/rock samples best characterize the average $\delta^{13}C$ of the total carbonate produced and preserved in the marine system (Shackleton, 1987).

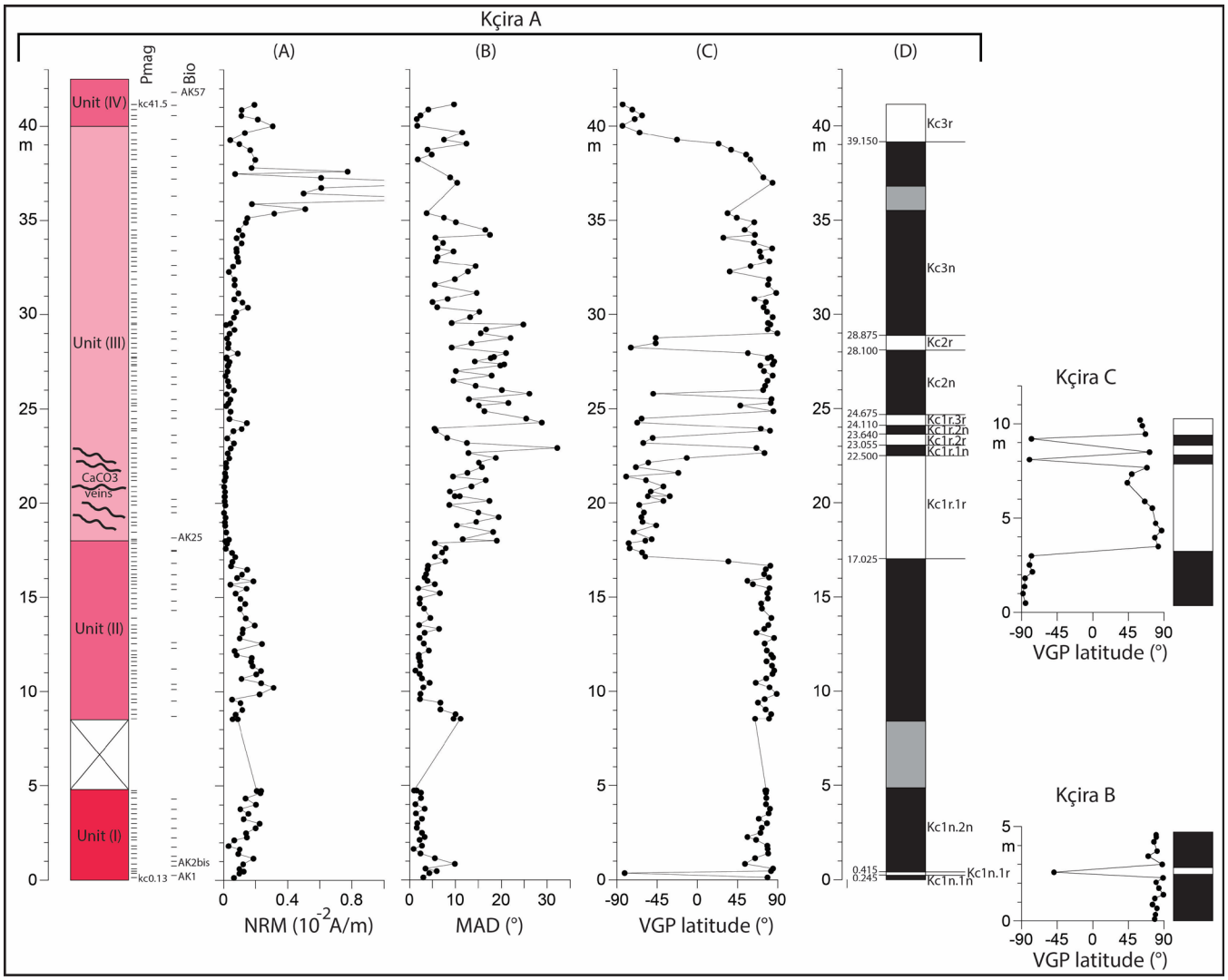

Figure 6 – Paleomagnetic properties of Kçira-A, Kçira-B, and Kçira-C samples. For Kçira-A. ***A***, Natural remanent magnetization (NRM). **B**, Mean angular deviation (MAD) of the characteristic Ch component. ***C***, Relative virtual geomagnetic pole (VGP) latitudes of the characteristic Ch component. ***D***, Magnetic polarity interpretation with filled (open) bars representing normal (reverse) polarity; single-sample polarity zones are shown by half bars. Also reported are the VGP latitudes and magnetic polarity zones of Kçira-B and Kçira-C (data from Muttoni et al., 1996).

DISCUSSION AND FUTURE DIRECTIONS

In virtue of its stratigraphic continuity, quality of magnetostratigraphic and biostratigraphic (especially conodonts) records, promising chemostratigraphic data, relatively simple accessibility (130 km by car from the capital city Tirana and near a village with accommodations and provisions), and logistics support provided by the Geological Survey of Albania, we consider Kçira-A a reliable GSSP to define the base of the Anisian. Potential events under scrutiny and critical discussion to define the base Anisian include at present both biostratigraphic and magnetostratigraphic datums (Fig. 8):

1. The FO of *Gladigondolella tethydis* at meter 15.70 (sample AK20).

2. The FO of *Chiosella timorensis* at meter 22.40 (sample AK30).

3. The last occurrence (LO) of *Gladigondolella carinata* at meter 26.30 (sample AK36), albeit this conodont has at present a very discuntinuous distribution at Kçira-A (Fig. 8).

4. The base of magnetozone Kc1r.1r at meter 17.025.

5. The base of magnetozone Kc1r.1n (= MT1n of Hounslow et al., 2007) at meter 22.50 close to the FO of *Chiosella timorensis* at meter 22.40.

6. The base of magnetozone Kc2n at meter 24.675.

Aside magnetostratigraphy that is already well-resolved (Muttoni et al., 1996), these and/or possibly other biostratigraphic events potentially useful to approximate the base of the Anisian would need to be re-assessed and better defined with additional sampling at Kçira-A to demonstrate their ability for global correlation. Dedicated sampling would also be needed to provide the section with a continuous $\delta^{13}C$ and $\delta^{18}O$ record coupled with microfacies analysis.

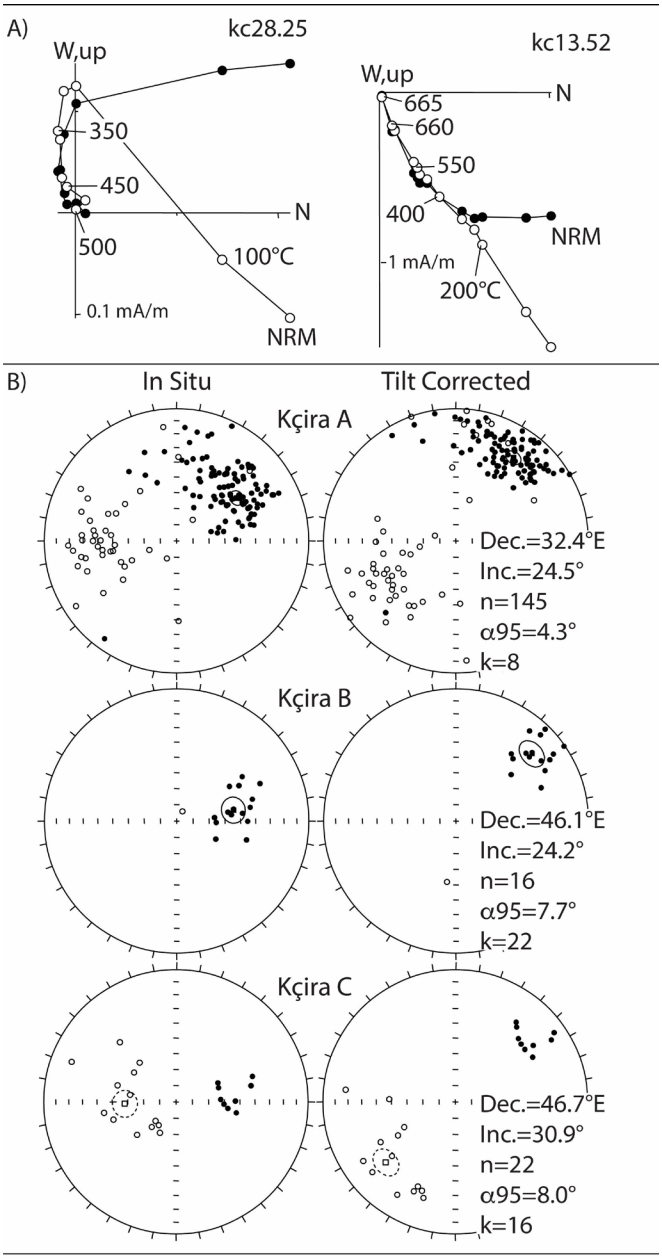

Figure 7 – Paleomagnetic properties of Kçira-A, Kçira-B, and Kçira-C samples. ***A***, Zijderveld thermal demagnetograms of representative samples from Kçira-A. Closed symbols are projections onto the horizontal plane and open symbols are projections onto the vertical plane in in situ coordinates and demagnetization temperatures are expressed in °C. ***B***, Equal-area projections before (in situ) and after bedding tilt correction of the characteristic Ch component directions from Kçira-A, Kçira-B, and Kçira-C, with associated site-mean directions calculated with standard Fisher statistics (data from Muttoni et al., 1996).

ACKNOWLEDGEMENTS

Mark Hounslow and Christopher McRoberts are thanked for comments on earlier versions of this manuscript. Digital listings of data can be made available upon request to the corresponding author.

REFERENCES

Arthaber, G. von 1911. Die Trias von Albanien. Beiträge zur Paläontologie Österreich-Ungarns, 24: 169–277.

Balini, M. & Nicora, A. 1998. Stop 3.3°: Conodonts from the Pelsonian-Illyrian Section of Dont (Zoldo Valley, Belluno). *In*, Perri M. C. & Spalletta C. (eds.), ECOS VII Southern Alps Field Trip Guidebook. Giornale di Geologia, Serie 3, 60: 260–267.

Budurov, K. & Stefanov, S. 1972. Plattform-Conodonten und ihre Zonen in der mittleren Trias Bulgariens. Mitteilungen der Gesellschaft der Geologie und Bergbaustudenten in Österreich, 21: 829–852.

Budurov, K. & Stefanov, S. 1975. Neue Daten uber die Conodonten-Chronologie der balkaniden mittleren Trias. Comptes Rendus de l'Académie Bulgare des Sciences, 28: 791–794.

Coplen, T. B. 1995. Discontinuance of SMOW and PDB. Nature, 375: 285.

Cramer, B. D., & Saltzman, M. R. 2005. Sequestration of ^{12}C in the deep ocean during the early Wenlock (Silurian) positive carbon isotope excursion. Palaeogeography, Palaeoceanography, Palaeoclimatology, 219: 333–349.

Epstein, A. G., Epstein, J. B., & Harris, L. D. 1977. Conodont color alteration: an index to organic metamorphism. U.S. Geological Survey, Professional Paper, 995, 36 pp.

Farabegoli, E. & Perri, M. C. 1998. Stop 3.3B: Middle Triassic conodonts at the Pelsonian/ Illyrian boundary of the Nosgieda section (Southern Alps, Italy). *In*, Perri M. C. & Spalletta C. (eds.), ECOS VII Southern Alps Field Trip Guidebook. Giornale di Geologia, Serie 3, 60: 268–274.

Gaetani, M., Jacobshagen, V., Nicora, A., Kauffmann, G., Tselepidis, V., Sestini, N. F., Mertmann, D. & Skourtsis-Coroneou, V. 1992. The Early-Middle Triassic boundary at Chios (Greece). Rivista Italiana di Paleontologia e Stratigrafia., 98: 181–204.

Gaetani, M., Meço, S., Rettori, R., Henderson, C. M. & Tulone, A. 2015. The Permian and Triassic in the Albanian Alps. Acta Geologica Polonica, 65(3): 271–295.

Gawlick, H.-J., Goričan, Š., Missoni, S., Dumitrica, P., Lein, R., Frisch, W. & Hoxha. L. 2016. Middle and Upper Triassic radiolarite components from the Kçira-Dushi-Komani ophiolitic mélange and their provenance (Mirdita Zone, Albania). Revue de Micropaléontologie, 59(4): 359–380.

Gawlick, H.-J., Frisch, W., Hoxha, L., Dumitrica, P., Krystyn, L., Lein, R., Missoni, S. & Schlagintweit, F. 2008. Mirdita Zone ophiolites and associated sediments in Albania reveal Neotethys Ocean origin. International Journal of Earth Sciences, 97(4): 865.

Gawlick, H., Lein, R., Missoni, S., Krystyn, L., Frisch, W. & Hoxha, L. 2014. The radiolaritic-argillaceous Kcira-Dushi-Komani sub-ophiolithic Hallstatt Mélange in the Mirdita Zone of Northern Albania. Buletini i Shkencave Gjeologjike, Spec. Issue, 4: 1–32.

Gedik, I. 1975. Die Conodonten der Trias auf der Kocaeli-Halbinsel (Türkey). Palaeontographica, 150: 99–160.

Germani, D. 1997. New data on ammonoids and biostratigraphy

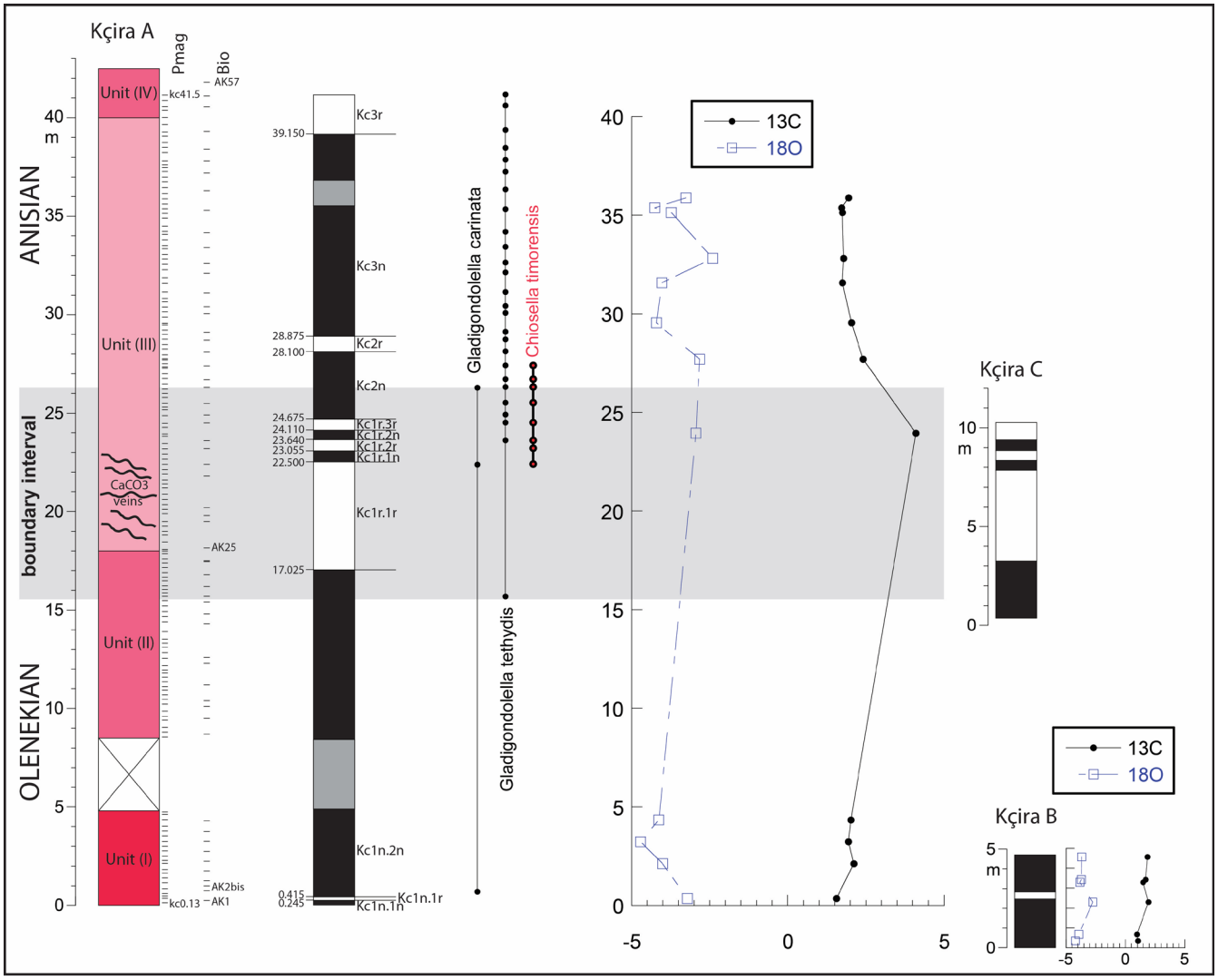

Figure 8 – Summary of magnetostratigraphic and key biostratigraphic events at Kçira-A across the Olenekian–Anisian boundary interval. Also shown are the magnetic stratigraphies of Kçira-B and Kçira-C, as well as the bulk C and O isotopes pilot data from Kçira-A and Kçira-B.

of the classical Spathian Kçira sections (Lower Triassic, Albania). Rivista Italiana di Paleontologia e Stratigrafia, 103(3): 267–292.

Grădinaru, E., Kozur, H., Nicora, A. & Orchard, M. J. 2006. The *Chiosella timorensis* lineage and correlation of the ammonoids and conodonts around the base of the Anisian in the GSSP candidate at Deşli Caira (North Dobrogea, Romania). Albertiana, 34: 34–38.

Grădinaru, E., Orchard, M. J., Nicora, A., Gallet, Y., Besse, J., Krystyn, L., Sobolev, E. S., Atudorei, V. & Ivanova, D. 2007. The Global Boundary Stratotype Section and Point (GSSP) for the base of the Anisian Stage: Deşli Caira Hill, North Dobrogea, Romania. Albertiana, 36: 54–71.

Guex, J., Hungerbühler, A., Jenks, J. F., O'Dogherty, L., Atudorei V., Taylor, D. G., Bucher, H. & Bartolini, A. 2010. Spathian (Lower Triassic) ammonoids from western USA (Idaho, California, Utah and Nevada). Mémoires de Géologie (Lausanne), 49: 1–211.

Hounslow, M.W., Szurlies, M., Muttoni, G. & Nawrocki, J. 2007. The magnetostratigraphy of the Olenekian-Anisian boundary and a proposal to define the base of the Anisian using a magnetozone datum. Albertiana 36: 72–77.

Jenks, J., Guex, J., Hungerbühler, A., Taylor, D. G. & Bucher, H. 2013. Ammonoid biostratigraphy of the early Spathian *Columbites parisianus* Zone (Early Triassic) at Bear Lake Hot Springs, Idaho. *In*, Tanner, L. H., Spielmann, J. A. & Lucas, S. G. (eds.), 2013, The Triassic System. New Mexico Museum of Natural History and Science Bulletin, 61: 268–283.

Knobbe, T. K., & Schaller, M. F. 2018. A tight coupling between atmospheric pCO_2 and sea-surface temperature in the Late Triassic. Geology, 46: 43–46.

Kovacs, S. & Kozur, H. 1980. Stratigraphische Reichweite der wichtigsten Conodonten (ohne Zahnreichen conodonten) der Mittel- und Obertrias. Geologisch-Paläontologische Mitteilungen Innsbruck, 10: 47–78.

Kovacs, S. & Ralisch-Felgenhauer, E. 2005. Middle anisian (Pelsonian) platform conodonts from the Triassic of the Mecsek Mts. (South Hungary) – Their taxonomy and

stratigraphic significance. Acta Geologica Hungarica, 48: 69–105

Kozur, H., Mostler, H. & Krainer, K. 1998. *Sweetospathodus* n. gen. and *Triassospathodus* n. gen., Two important Lower Triassic Conodont Genera. Geologia Croatica, 51: 1–5.

Lehrmann, D. J., Stepchinski, L., Altiner, D., Orchard, M. J., Montgomery, P., Enos, P., Elwood, B. B., Bowring, S. A., Ramezani, J., Wang, H., Wei, J., Yu, M., Griffiths, J. D., Minzoni, M., Schaal, E. K., Li, X., Meyer, K. M. & Payne, J. L. 2015. An integrated biostratigraphy (conodonts and foraminifers) and chronostratigraphy (paleomagnetic reversals, magnetic susceptibility, elemental chemistry, carbon isotopes and geochronology) for the Permian-Upper Triassic strata of Guandao section, Nanpanjiang Basin, South China. Journal of Asian Earth Sciences, 108: 117–135.

Maron, M., Muttoni, G., Rigo, M., Gianolla, P. & Kent D. V. 2019. New magnetobiostratigraphic results from the Ladinian of the Dolomites and implications for the Triassic geomagnetic polarity timescale. Palaeogeography, Palaeoclimatology, Palaeoecology, 517, 52–73.

Marshall, J. D. 1992. Climatic and oceanographic isotopic signals from the carbonate rock record and their preservation. Geological Magazine, 129: 143–160.

Meço, S. 2010. Litho-biostratigraphy and the conodonts of Palaeozoic/Triassic deposits in Albania. Palaeontographica Abteilung, A: 131–197.

Meço, S. & Aliaj, S. 2000. Geology of Albania. Beiträge zur Regionalen Geologie der Erde, Gebrüder Borntraeger Verlagsbuchhandlung, 246 pp.

Mosher, L. C. 1970. New conodont species as Triassic fossil guide. Journal of Paleontology, 42: 947–954.

Muttoni, G., Kent, D. V., Meço, S., Nicora, A., Gaetani, M., Balini, M., Germani, D. & Rettori, R. 1996. Magneto-biostratigraphy of the Spathian to Anisian (Lower to Middle Triassic) Kçira Section, Albania. Geophysical Journal International, 127: 503–514.

Muttoni, G., Kent, D. V. & Gaetani, M. 1995. Magnetostratigraphy of a Lower-Middle Triassic boundary section from Chios (Greece). Physics of the Earth and Planetary Interiors, 92: 245–261.

Muttoni, G., Mazza, M., Mosher, D., Katz, M. E., Kent, D. V., Balini, M. 2014. A Middle– Late Triassic (Ladinian–Rhaetian) carbon and oxygen isotope record from the Tethyan Ocean. Palaeogeography, Palaeoclimatology, Palaeoecology, 399: 246–259.

Nicora, A. 1977. Lower Anisian platform-conodonts from the Tethys and Nevada: taxonomic and stratigraphic revision. Palaeontographica, 157: 88–107.

Nopcsa, F. 1929. Geologie und Geographie Nordalbaniens. Geologica Hungarica, Series Geologica, 3: 1–620.

Orchard, M. J. 1995. Taxonomy and correlation of Lower Triassic (Spathian) seminate conodonts from Oman and revision of some species of *Neospathodus*. Journal of Paleontology, 69: 110–122.

Orchard, M. J., Grădinaru, E. & Nicora, A. 2007a. A summary of the conodont succession around the Olenekian-Anisian boundary at Deşli Caira, North Dobrogea, Romania. *In*, Lucas, S. G. & Spielmann, J. A. (eds.), The Global Triassic. New Mexico Museum of Natural History and Science Bulletin, 41: 34–345.

Orchard, M. J., Lehrmann, D. J., Jiayong, W., Hongmei, W. & Taylor, H. 2007b. Conodonts from the Olenekian-Anisian boundary beds, Guandao, Guizhou Provice, China. *In*, Lucas, S. G. & Spielmann, J. A. (eds.), The Global Triassic. New Mexico Museum of Natural His¬tory and Science Bulletin, 41: 347–354.

Richoz, S., Krystyn, L., Horacek, M. & Spötl, C. 2007. Carbon isotope record of the Induan-Olenekian candidate GSSP Mud and comparison with other sections. Albertiana, 35: 35–40.

Saltzman, M. R. & Thomas, E. 2012. Carbon isotope stratigraphy. *In*, Gradstein, F. M., Ogg, J. G., Schmitz, M. & Ogg, G. (eds.), The Geologic Time Scale 2012: Boston, Massachusetts, Elsevier, p. 207–232.

Shackleton, N. J. 1987. Oxygen isotopes, ice volume and sea level. Quaternary Science Reviews, 6: 183–190.

Sudar, M. & Budurov, K. 1979. New conodonts from the Triassic in Yugoslavia and Bulgaria. Geologica Balcanica, 9: 47–52.

Sudar, M. N., Gawlick, H.-J., Lein, R., Missoni, S., Kovacs, S. & Jovanović, D. 2013. Depositional environment, age and facies of the Middle Triassic Bulog and Rid formations in the Inner Dinarides (Zlatibor Mountain, SW Serbia): evidence for the Anisian break-up of the Neotethys Ocean. Neues Jahrbuch für Geologie und Paläontologie-Abhandlungen, 269(3): 291–320.

Trotter, J. A., Williams, I. S., Nicora, A., Mazza, M. & Rigo, M. 2015. Long-term cycles of Triassic climate change: a new $\delta^{18}O$ record from conodont apatite. Earth and Planetary Science Letters, 415: 165–174.

Veizer, J. & Prokoph, A. 2015. Temperatures and oxygen isotopic composition of Phanerozoic oceans. Earth-Science Reviews, 146: 92–104.